

FAST COMMUNICATION
THREE-DIMENSIONAL LOCALIZED SOLITARY
GRAVITY-CAPILLARY WAVES *

PAUL A. MILEWSKI[†]

Abstract. In a weakly nonlinear model equation for capillary–gravity water waves on a two-dimensional free surface, we show, numerically, that there exist localized solitary traveling waves for a range of parameters spanning from the long wave limit (with Bond number $B > 1/3$, in the regime of the Kadomtsev-Petviashvili-I equation) to the wavepacket limit ($B < 1/3$, in the Davey-Stewartson regime). In fact, we show that these two regimes are connected with a single continuous solution branch of nonlinear localized solitary solutions crossing $B = 1/3$.

Key words. three-dimensional, solitary wave, lumps, capillary–gravity.

AMS subject classifications. 76B45, 76B25, 76B15

1. Introduction

There has been considerable computational, experimental and theoretical work on localized solitary water waves on a one-dimensional free surface. For gravity waves, the celebrated shallow water Korteweg-de Vries solitons, and their (numerical) extensions to the full Euler equations are well known [4]. There are also well known solitary capillary-gravity waves, either of the Korteweg –de Vries type (albeit of depression) when the depth is very small compared to the surface tension length scale, or of wavepacket type when the depth is larger (or infinite) [8, 16, 4, 12, 7]. For a two-dimensional free-surface (three-dimensional fluid) there is considerably less work on the subject of localized solitary waves. With gravity alone, localized waves can be ruled out (by the physical argument herein or, rigorously for the full Euler equations in [3]). For capillary gravity waves, physical arguments do not rule out localized solutions. In the regime of small depth compared to the surface tension length scale, the Kadomtsev-Petviashvili-I equation is the generalization of the Korteweg–de Vries equation, and it supports solitary “lump” solutions [14, 2]. Recently these solutions have been shown to exist in full Euler equations in [5]. In a deeper water regime there is so far little evidence that solitary localized waves exist. In this paper we find such localized solitary waves in deeper water for an equation derived from a small amplitude expansion of the three-dimensional free surface problem. We compute them numerically by finding a continuous branch of solutions linking KP-I-like lumps and the new waves of wavepacket type. (This continuous branch exists also for the one-dimensional free surface problem.) Furthermore, given that there appears to be no bifurcations on the branch of solutions linking shallow lumps to deeper water lumps, we think that these waves are stable. We also believe that the full Euler equations should support capillary–gravity localized solitary waves in deeper water.

Traveling solitary waves in weakly nonlinear regimes of 1+1 dimensional dispersive wave equations are usually of two types: long waves that bifurcate from linear solutions near $k = 0$ (k is the Fourier wavenumber), and which are usually described by solitary solutions of Korteweg-de Vries or other long wave equations (see Figure

*Received: September 6, 2004; accepted (in revised version): November 16, 2004. Communicated by Lenya Ryzhik.

[†]Department of Mathematics, University of Wisconsin, 480 Lincoln Dr., Madison, WI 53706 (milewski@math.wisc.edu). Paul Milewski is partially supported by NSF-DMS.

3.2 left panel), and those which bifurcate from a local extremum of the phase velocity $c(k)$ at finite k . At this wavenumber,

$$0 = c'(k) = \left(\frac{\omega(k)}{k} \right)' = \frac{\omega'(k)}{k} - \frac{\omega(k)}{k^2} = \frac{1}{k}(c_g - c), \quad (1.1)$$

implying that $c_g = c$. This allows a modulation envelope and its carrier wave to travel at the same speed, creating a traveling “wavepacket” solitary wave [1] (see Figure 3.2 right panel for an example). These are usually described by a Nonlinear Schrödinger or other modulation-type equation. Both of these types of solutions exist in water waves [4]. Note that, despite the fact that long solitary waves bifurcating from $k=0$ look different from wavepacket solitary waves, a linear wave near $k=0$ (with $\omega(0)=0$) also has equal phase and group velocity.

In 2+1 dimensions one may ask whether spatially localized solitary waves (waves which decay to zero in both spatial directions—not only in the direction of propagation) exist in a particular problem. A physically motivated necessary condition for this is that there exist no other linear modes (other than the mode from which the wave bifurcates) resonant with the speed of the solitary wave. If such a resonance is present, the small amplitude “periphery” of the traveling wave would radiate energy away and thus destroy its coherence.

This condition means that a localized nonlinear traveling wave may bifurcate from a particular wavevector \mathbf{k}^* with $\mathbf{c}^* = \frac{\omega(\mathbf{k}^*)}{|\mathbf{k}^*|^2} \mathbf{k}^*$ only if

$$\omega(\mathbf{k}) - \mathbf{c}^* \cdot \mathbf{k} = 0, \text{ has no solutions for } \mathbf{k} \neq \mathbf{k}^*. \quad (1.2)$$

This condition can be satisfied at $\mathbf{k}^* = \mathbf{0}$ or at finite \mathbf{k}^* . If it is satisfied locally near a wavenumber \mathbf{k}^* , clearly, it implies that there, $\mathbf{c}_g = \mathbf{c}$. However $\mathbf{c}_g = \mathbf{c}$ at a point does not imply (1.2). We refer the reader to Section 4 for a graphical interpretation of (1.2).

Note that (1.2) is satisfied *locally*, that is, near \mathbf{k}^* , in both 1+1 dimensional cases described above. In fact in 1+1 dimensions satisfying (1.2) is equivalent to $c(k)$ having an extremum. This is not the case in 2+1 dimensions, where the phase speed may have an extremum without (1.2) being satisfied (as in deep water gravity waves near $\mathbf{k}^* = 0$). Lastly, in 1+1 dimensions, if (1.2) is satisfied locally but not globally, then there may exist “generalised” solitary waves—waves with nondecaying oscillations at infinity.

If condition (1.2) is satisfied for a 2+1 dimensional problem, one can then explicitly seek traveling solutions, eliminating an independent variable, and reducing the problem to finding localized solutions to an equation in 2 spatial dimensions.

We shall consider here the problem of capillary-gravity waves in a fluid of finite depth modeled by the weakly nonlinear equations

$$u_{tt} + (1 - B\Delta)\mathcal{L}u + \epsilon\mathcal{N}(u) = 0 \quad (1.3)$$

with

$$\mathcal{L} = (-\Delta)^{\frac{1}{2}} \tanh \left[(-\Delta)^{\frac{1}{2}} \right] \quad (1.4)$$

and

$$\begin{aligned} \mathcal{N} = & (1 - B\Delta) (\nabla \cdot (\nabla u (1 - B\Delta)^{-1} u_t)) + \frac{1}{2} (\nabla u)_t^2 \\ & + (\mathcal{L}u)_t^2 + ((1 - B\Delta)\mathcal{L}^2 u) ((1 - B\Delta)^{-1} u_t). \end{aligned} \quad (1.5)$$

Here, $\epsilon = a/H \ll 1$, the ratio of wave amplitude to depth and $B = \gamma/H^2$ is the depth based Bond number, the ratio of the surface tension coefficient to the depth squared. The dispersion relation of the linear problem is the well known finite depth capillary-gravity relation

$$\omega^2 = |\mathbf{k}| \tanh(|\mathbf{k}|) (1 + B\mathbf{k}^2). \quad (1.6)$$

The water surface is given by $H(1 + \epsilon\eta(x, y, t))$, where, to leading order,

$$(1 - B\Delta)\eta = -u_t. \quad (1.7)$$

This paper is organized as follows: in Section 2 we briefly derive the governing equations. In Section 3 we describe the possible long and wavepacket travelling solutions for a one-dimensional free surface, and show numerically that these two are, in fact, part of the same nonlinear solution branch. In Section 3 we extend the results to a two-dimensional free surface, and find new localized two-dimensional wavepacket solitary waves for values of $B < 1/3$. We show also that they are connected by a nonlinear solution branch to long localized solitary waves of the KP-I equation.

2. Gravity-Capillary Finite Depth Equations

We give a brief derivation of our small amplitude gravity-capillary wave equation for water of finite depth. The method is similar to that of [10, 2, 13]. We first derive the form appropriate for the deep water limit and describe the different scalings needed for the equation more appropriate for the shallow water limit (1.3).

Given a surface tension coefficient γ , an undisturbed fluid depth H , and a typical wave amplitude a , then using $\gamma^{1/2}$ as the length scale, a as the scale for typical free surface displacements, $a\gamma^{1/4}g^{1/2}$ as the velocity potential scale, $\gamma^{1/4}g^{-1/2}$ as the time scale, the dimensionless inviscid, irrotational water wave equations can be written in terms of the velocity potential $\phi(x, y, z, t)$ and free surface displacement $\eta(x, y, t)$ with unit normal $\hat{\mathbf{n}}$ as

$$\Delta\phi + \phi_{zz} = 0, \quad 0 < z < b + \epsilon\eta, \quad (2.1)$$

$$\phi_z = 0, \quad z = 0, \quad (2.2)$$

$$\eta_t + \epsilon(\nabla\eta \cdot \nabla\phi) - \phi_z = 0, \quad z = b + \epsilon\eta, \quad (2.3)$$

$$\phi_t + \epsilon\frac{1}{2}(\nabla\phi)^2 + \epsilon\frac{1}{2}\phi_z^2 + \eta - \nabla \cdot \hat{\mathbf{n}} = 0, \quad z = b + \epsilon\eta. \quad (2.4)$$

Expanding the two surface boundary conditions about $z = b$, and eliminating η , leads to a single boundary condition in ϕ at $z = b$, correct to $O(\epsilon)$:

$$\phi_{tt} + (1 - \Delta)\phi_z + \epsilon\mathcal{Q}(\phi) = 0, \quad z = b \quad (2.5)$$

where

$$\begin{aligned} \mathcal{Q} = & (1 - \Delta)(\nabla \cdot (\nabla\phi(1 - \Delta)^{-1}\phi_t)) + \frac{1}{2}(\nabla\phi)_t^2 \\ & + \frac{1}{2}(\phi_z)_t^2 - (\phi_{tz}(1 - \Delta)^{-1}\phi_t)_t. \end{aligned} \quad (2.6)$$

Next, we solve Laplace's equation with the bottom boundary condition, obtaining

$$\phi(x, y, z, t) = \cosh \left[z(-\Delta)^{\frac{1}{2}} \right] \Phi(x, y, t), \quad (2.7)$$

with

$$u(x, y, t) = \phi(x, y, b, t) = \cosh \left[b(-\Delta)^{\frac{1}{2}} \right] \Phi(x, y, t) \quad (2.8)$$

being the velocity potential at $z = b$. With this notation, it follows that $\phi_z(x, y, b, t) = \mathcal{L}u$ and where \mathcal{L} is defined as $\mathcal{L} = (-\Delta)^{\frac{1}{2}} \tanh \left[b(-\Delta)^{\frac{1}{2}} \right]$ and has the symbol $\hat{\mathcal{L}}(\mathbf{k}) = |\mathbf{k}| \tanh(b|\mathbf{k}|)$. Thus if $\hat{u}(\mathbf{k}, t)$ is the Fourier transform of $u(\mathbf{x}, t)$, then

$$\mathcal{L}u = \frac{1}{2\pi} \int_{-\infty}^{\infty} |\mathbf{k}| \tanh(b|\mathbf{k}|) e^{i\mathbf{k}\cdot\mathbf{x}} \hat{u}(\mathbf{k}, t) d\mathbf{k}. \quad (2.9)$$

Substitution of (2.7) into the boundary condition (2.5) yields, after some simplification, the equation

$$u_{tt} + (1 - \Delta) \mathcal{L}u + \epsilon \mathcal{N}(u) = 0 \quad (2.10)$$

with

$$\begin{aligned} \mathcal{N} = & (1 - \Delta) (\nabla \cdot (\nabla u (1 - \Delta)^{-1} u_t)) + \frac{1}{2} (\nabla u)_t^2 \\ & + (\mathcal{L}u)_t^2 + ((1 - \Delta) \mathcal{L}^2 u) ((1 - \Delta)^{-1} u_t). \end{aligned} \quad (2.11)$$

Here, $\epsilon = a/\sqrt{\gamma} \ll 1$ is the ratio of wave amplitude a to characteristic capillary scale $\sqrt{\gamma}$, $b = H/\sqrt{\gamma}$ is the inverse square-root Bond number, and $u(x, y, t)$ is the velocity potential at the undisturbed free surface. The dispersion relation obtained by setting $\epsilon = 0$ in (2.10) is the familiar

$$\omega^2 = |\mathbf{k}| \tanh(b|\mathbf{k}|) (1 + \mathbf{k}^2). \quad (2.12)$$

The water surface is given by $b + \epsilon \eta(x, y, t)$, where to leading order, η can be obtained by inverting

$$(1 - \Delta) \eta = -u_t. \quad (2.13)$$

Another possible nondimensionalization of the equations is based on using depth as a length scale. Choosing H as the length scale, a as the scale for typical free surface displacements, $a(gH)^{1/2}$ as the velocity potential scale, $(H/g)^{1/2}$ as the time scale. Proceeding as above, one obtains the equations (1.3–1.7).

In practice, (2.10–2.13) is more appropriate for capillary waves in deeper water since we can fix γ and take the limit $H, b \rightarrow \infty$, whereas (1.3–1.7) is more appropriate for shallow water, when the surface tension coefficient varies.

Many further simplifications of these equations are possible. In particular, for long waves, expanding for small wavenumber and truncating at sixth order, one obtains from (1.3), the approximate Benney-Luke type equation

$$u_{tt} - \Delta u + \left(B - \frac{1}{3} \right) \Delta^2 u - \left(\frac{2}{15} - \frac{B}{3} \right) \Delta^3 u + \epsilon [(\nabla u)_t^2 + u_t \Delta u] = 0. \quad (2.14)$$

We shall use this equation, because as we shall see, it captures the right form for the dispersion relation and nonlinearity of (1.3) in the regimes that interest us.

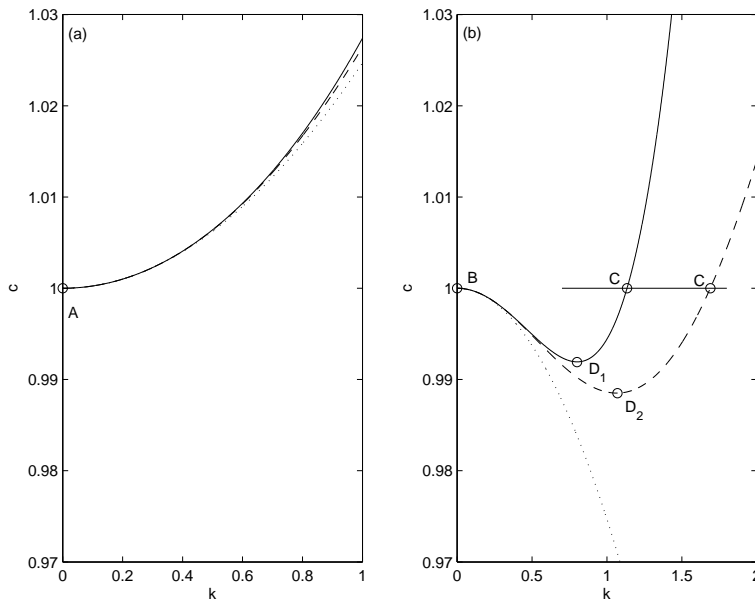


FIG. 3.1. Phase speed plots for linearized equations 3.3 (solid) and 3.1 (dot) and 1.3 (dashed) for (a) $B = 1/3 + 1/20$, (b) $B = 1/3 - 1/20$.

3. One Dimensional Free Surface

For a one dimensional free surface one can write from (2.14), and upon further truncation, a Boussinesq equation:

$$u_{tt} - u_{xx} + \left(B - \frac{1}{3}\right) u_{xxxx} + 2u_x u_{xt} + u_t u_{xx} = 0. \quad (3.1)$$

The Korteweg-de Vries (KdV) equation is easily obtained from (3.1) by seeking solutions traveling one-way. We have taken $\epsilon = 1$ for simplicity, that is, we incorporate ϵ into the solution u and seek solutions with small norm. This Boussinesq equation has the well known sech^2 solitary wave solutions, given by

$$u_x = a \text{sech}^2[\kappa(x - ct)], \quad c^2 = 1 - 4\left(B - \frac{1}{3}\right)\kappa^2, \quad a = \frac{c^2 - 1}{c}. \quad (3.2)$$

In this approximation, (1.7) implies $\eta = -u_t = cu_x$. Thus, for right-traveling waves ($c > 0$), if $B < 1/3$, the waves are of elevation and if $B > 1/3$, they are of depression. For water, $\gamma = 7.2 \times 10^{-6} m^2$ and $B = 1/3$ corresponds to waves on a fluid of depth $H \approx 0.5 cm$. This small depth is often cited as a reason for the physical irrelevance of this regime, since at such small depths viscous effects are important.

The inclusion of the sixth derivative term of (2.14) to (3.1) yields the sixth order Boussinesq equation

$$u_{tt} - u_{xx} + \left(B - \frac{1}{3}\right) u_{xxxx} + \left(\frac{2}{15} - \frac{B}{3}\right) u_{xxxxx} + 2u_x u_{xt} + u_t u_{xx} = 0, \quad (3.3)$$

which is asymptotically correct for $B \approx 1/3$ since both dispersive terms can be formally made to have the same order [11]. The higher derivative term changes the waves of

elevation and depression in different ways, and allows for the possibility of wavepacket solitary waves as we describe below. (We restrict here $B < 6/15$ to fix the sign of the sixth derivative term so that the dispersion relation is qualitatively similar to the full problem.) The dispersion relations for the fourth-order Boussinesq (3.1), sixth-order Boussinesq (3.3), and the full problem (1.3) are shown in Figure 3.1 for $B < 1/3$ and $B > 1/3$.

For $B > 1/3$ in Figure 3.1(a), the dispersion relation does not qualitatively change for the three cases, and the solitary waves of depression (3.2) which bifurcate from point A are similar to each other (see Figure 3.2, leftmost plot). For $B < 1/3$ in Figure 3.1(b), the dispersion relation changes substantially from the addition of the sixth derivative terms, and one should either use a sixth-order Boussinesq or a full-dispersion weakly nonlinear equation such as (1.3). These two equations for a Bond number close to $1/3$ and small nonlinearities are qualitatively similar. The solitary waves of elevation (3.2) which bifurcate from point B are now resonant with the shorter wave at points C (i.e. the condition (1.2) is satisfied only locally at B but not globally), and thus exhibit nondecaying oscillations. These waves, with exponentially small (due to the smoothness of the main wave [9]) tails, are usually called generalized solitary waves. However, in Figure 3.1(b) there is also a new family of wavepacket solitary waves, bifurcating from the minima of $c(k)$ at points D_1 or D_2 . Since, as B is increased towards $1/3$, the D 's move toward the origin, it is reasonable to expect that this branch of solitary waves is connected to the branch of depression waves at point A .

The preceding discussion was based completely on the linear dispersion relation. We shall establish numerically that the nonlinear terms support solitary waves.

This is indeed the case, as can be seen in Figure 3.2. It shows a sequence of solitary traveling wave solutions obtained by a continuation method by fixing the norm of the solution and varying B in the sixth-order Boussinesq (3.3). (B decreases from left to right in Figure 3.2.) The leftmost wave is obtained by using the solution (3.2) to (3.1) as an initial approximation. Note that we show u_x , which is proportional to the free surface displacement with $\eta = cu_x$ in this limit.

These solutions were computed by Newton's method on a Fourier spectral decomposition of the solution. Specifically, we expand solutions to (3.3) as

$$u(\theta) = \sum_{n=-N}^N a_n e^{in\kappa\theta}, \quad \theta = x - ct, \quad (3.4)$$

with $a_n = a_{-n}$ real. Thus we assume that the solution is real, symmetric about $x=0$, and periodic with period $2L = 2\pi/\kappa$. There are $N+2$ unknowns $a_j, j=0 \dots N$ and c . The $N+2$ equations are the N projections of (3.3) on $e^{in\theta}, j=1 \dots N$, the equation fixing $\|u_x\|_2$, and, setting $u(-L) = 0$. Typically, $N=128$ or 256 .

The rightmost solitary wave has a Fourier spectrum peak at $k \approx 0.9$ and corresponds to the point D_1 in Figure 3.1. If one would continue this solution branch by lowering the amplitude with B fixed, it would approach a carrier wave with an envelope solitary wave and $c \approx 0.977$ (the value of c at $k \approx 0.95$, the minimum D_1). The important conclusion is that there is a branch of solutions connecting the long solitary waves to wavepacket solitary waves. Lastly, we note that the solitary waves shown in Figure 3.2 are stable. In fact in [11] such waves are shown to be generated naturally in a model of flows over a bump.

We will now show that for two-dimensional free-surface waves this is also the case and we will be able to compute localized solitary two-dimensional wavepackets for

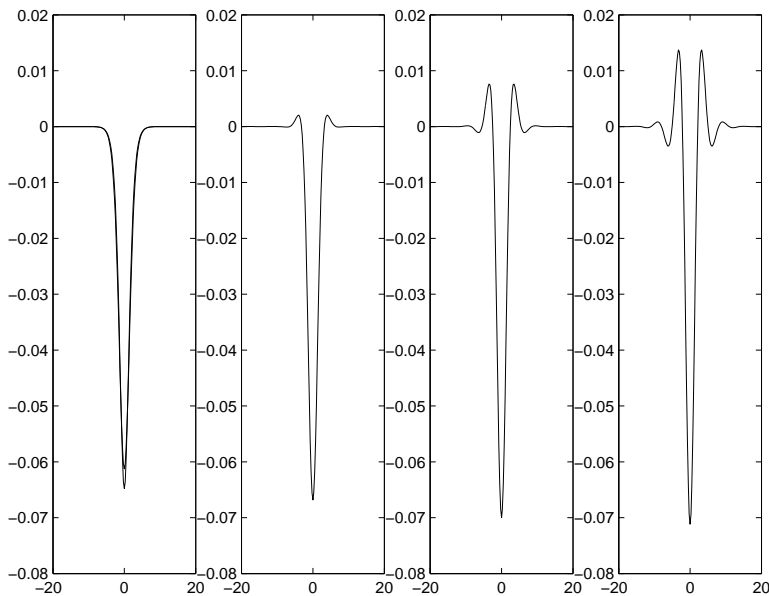


FIG. 3.2. Solitary waves of equation (3.3) (u_x is shown) for varying B . All solutions have $\|u_x\|_2=0.1$. From left to right: 1. $B=1/3+1/20$. The solution to (3.1) given by (3.2) ($c=0.9681$) and the solution to (3.3) ($c=0.9692$) are both shown and are almost identical. 2. $B=1/3$ ($c=0.9630$). 3. $B=1/3-1/20$ ($c=0.9556$). 4. $B=1/3-1/10$ ($c=0.9471$). Note that the scales are considerably stretched for emphasis, and that the computational domain was larger than is shown.

$B < 1/3$.

4. Two Dimensional Free Surface

We now focus our attention on two-dimensional, localized, solitary waves. We begin with the counterpart of the KdV equation for a two dimensional free surface, which is the Kadomtsev-Petviashvili (KP) equation

$$\left[\eta_t + \eta_x + \epsilon \left[\frac{3}{2} \eta \eta_x + \frac{1}{2} \left(\frac{1}{3} - B \right) \eta_{xxx} \right] \right]_x + \frac{1}{2} \eta_{yy} = 0. \quad (4.1)$$

This equation can be obtained from (2.14) by seeking one-way solutions with $y \rightarrow \epsilon^{1/2} y$, and further truncation. It was first derived in a study of the stability of KdV line solitons (the solution (3.2) with no variation in y) to slowly varying transverse perturbations. It turns out that for $B < 1/3$, line solitons are stable and that for $B > 1/3$ they are unstable. For $B > 1/3$ (the so-called KP-I equation) there also are solitary waves decaying in all directions, called lump solitons. These are given explicitly by

$$\eta = A \left[\frac{\frac{A}{8(B-1/3)}(x-ct)^2 + \frac{3A^2}{64(B-1/3)}\epsilon y^2 + 1}{\left[-\frac{A}{8(B-1/3)}(x-ct)^2 + \frac{3A^2}{64(B-1/3)}\epsilon y^2 + 1 \right]^2} \right], \quad c = 1 + \frac{3}{16}\epsilon A, \quad (4.2)$$

with $A < 0$. Note that these solutions decay only algebraically in x and y . Furthermore, there is numerical evidence that the instability of line solitons of KdV within

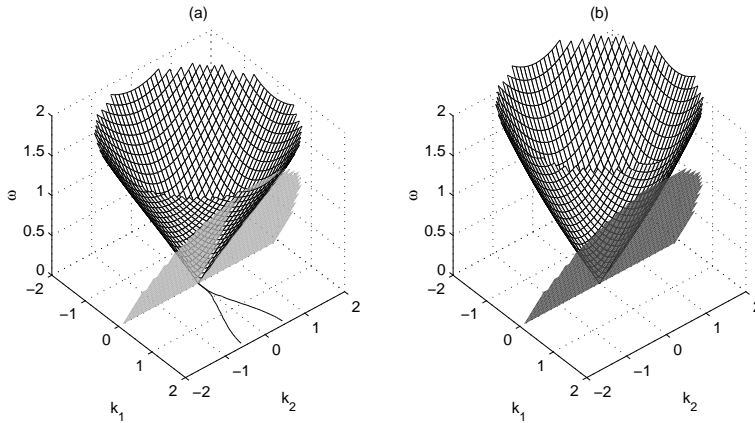


FIG. 4.1. Dispersion relation (1.6) and the plane $p = \mathbf{c} \cdot \mathbf{k}$ for $\mathbf{c} = (1, 0)$ at (a) $B = 1/3 - 1/10$. The curve on the \mathbf{k} plane is the projection of the point where p and ω intersect. (b) $B = 1/3 + 1/10$. There are no intersections of p and ω .

KP-I tend to produce such lump solitary waves. For $B < 1/3$, one obtains the KP-II equation which does not support localized solitary waves.

A simple argument for whether a nonlinear wave equation may support lump-like solitary waves, bifurcating from a point \mathbf{k}^* was given in the introduction (1.2). Graphically, (1.2) is equivalent to the dispersion surface $\omega(\mathbf{k})$ not intersecting the plane given by $p(\mathbf{k}) = \mathbf{c}^* \cdot \mathbf{k}$. For an isotropic dispersion relation where $\omega(|\mathbf{k}|)$, (1.2) is equivalent to $\omega/|\mathbf{k}|$ having a *minimum* at \mathbf{k}^* . Note that if $\omega/|\mathbf{k}|$ has a *maximum* the condition (1.2) will not be satisfied due to the surface $\omega(|\mathbf{k}|)$ not being locally convex, thus ruling out localized solitary waves. (For a 1+1 dimensional problem minima and maxima both permit solitary waves according to (1.2).)

This condition explains clearly why the KP equation (and the full dispersion relation (1.6)) can only support lumps bifurcating from $\mathbf{k}^* = 0$ (with $\mathbf{c} = (1, 0)$ in the scaling of (1.6)) for $B > 1/3$ and not for $B < 1/3$. This is shown graphically in Figure 4.1 using the full dispersion relation (1.6). For $B < 1/3$ there is a family of resonant linear waves, whereas for $B > 1/3$ there are none. If the dispersion relations for the KP equations were used instead, the results would be qualitatively similar. However, since the KP equations are not isotropic, the dispersion relations are not surfaces of revolution.

There is, however, the possibility of two-dimensional localized traveling waves for $B < 1/3$, bifurcating from finite \mathbf{k}^* in the problem with the full dispersion relation (1.6). This case is the two-dimensional equivalent to the solutions bifurcating from the minimum of c in Figure 3.2 (b). For example, Figure 4.2 shows that a plane through the origin and tangent to the bifurcation point does not have other intersections with the dispersion surface (1.6) for $B = 1/3 - 1/20$.

Furthermore, as B is increased towards $1/3$, this “wavepacket” lump bifurcation point tends to the KP-I bifurcation point $\mathbf{k}^* = 0$. Therefore, it is possible that the KP-I lumps for $B > 1/3$ can be continued into wavepacket lumps with $B < 1/3$ which would be in an “envelope equation” regime. The relevant envelope equation here is the Davey-Stewartson Equation, which has been shown to support localized *envelopes* [14], further indication that travelling localized solitary waves may be possible.

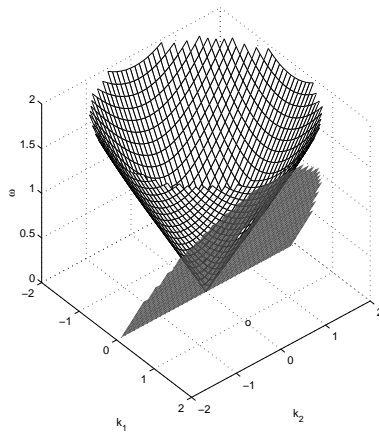


FIG. 4.2. Dispersion relation (1.6) and the plane $p = \mathbf{c} \cdot \mathbf{k}$ for $\mathbf{c} = (0.989, 0)$ at $B = 1/3 - 1/20$. The “o” on the \mathbf{k} plane is \mathbf{k}^* , the projection of the point where p and ω touch tangentially.

We note that these $B < 1/3$ wavepacket lumps would be more physically relevant than for $B > 1/3$, since, as B decreases, depth increases and viscous bottom effects become less important.

Within (2.14) we can indeed continue the KP-I lumps to wavepacket localized traveling waves with $B < 1/3$ as shown in Figure 4.3. The solution on the left is a solution to (2.14) with $B > 1/3$ obtained by using (4.2) as an initial approximation. This solution is very similar to the KP-I lump (see [13],[2]). The solution on the right is obtained by continuing this solution by varying B until $B < 1/3$. The solution has developed typical wavepacket oscillations in the x direction. We conjecture that the wavepacket solution is stable since it is connected on a continuous branch (no numerical evidence of bifurcations) to the KP-I solutions and these are known to be stable. Furthermore, in [2], KP-I-like lumps were numerically stable and shown to be generated in a model of shallow water flow over a localized bump in an equation similar to (2.14) for $B < 1/3$.

Computationally, the method is similar to that for one dimensional waves. We write solutions to (2.14)

$$u(\theta, y) = \sum_{m=-M}^M \sum_{n=-N}^N a_{m,n} e^{i(n\kappa_x \theta + m\kappa_y y)}, \quad \theta = x - ct, \quad (4.3)$$

with $a_{m,n} = a_{-m,n} = a_{m,-n}$ real. Thus the solution is real, symmetric with respect to both axes, and periodic on the rectangle of size $2L_x = 2\pi/\kappa_x$ by $2L_y = 2\pi/\kappa_y$. There are $(M+1)(N+1)+1$ unknowns, and we solve the equations obtained by projecting the spectrally truncated nonlinear terms of (2.14) on $e^{i(n\kappa_x \theta + m\kappa_y y)}$, $m = 0, \dots, M$, $n = 1, \dots, N$ (yielding $N(M+1)$ equations), by setting $u(-L_x, y) = 0$ (yielding $M+1$ equations), and by fixing $\|u_x\|_2$ (yielding one equation). Typical computations shown use $M, N = 64$.

Figure 4.4 shows the magnitude of the Fourier transform of the solutions in Figure 4.3. The figure shows clearly that the nature of the solution has changed from a “long” wave (with spectrum centered at $\mathbf{k} = \mathbf{0}$) to a “wavepacket” with spectrum centered at the point of tangency in Figure 4.2. The spectra also show that the

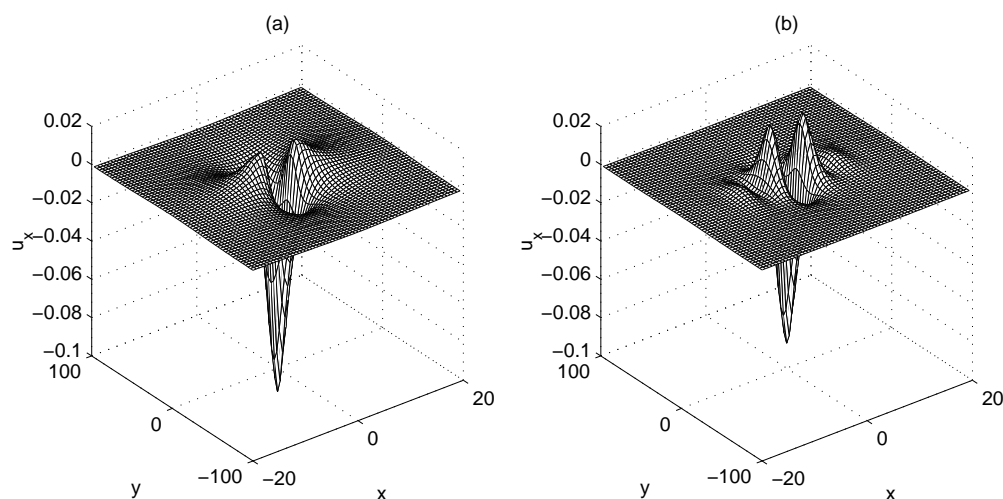


FIG. 4.3. Localized traveling solution to (2.14) (u_x shown, representing the free surface displacement) with $\|u_x\|_2 = 0.74$. (a) $B = 1/3 + 1/20$, with corresponding $c = 0.9743$. (b) $B = 1/3 - 1/10$, with $c = 0.9595$. The computational domain was 4 times larger to ensure decay at large x, y .

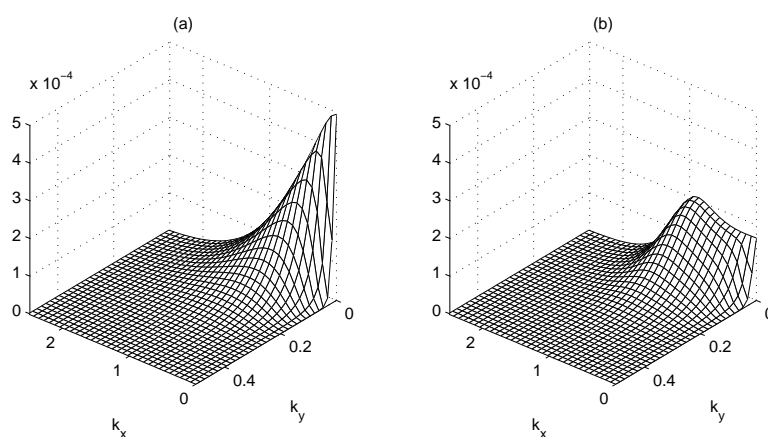


FIG. 4.4. Fourier spectra of the solutions shown in Figure 4.3. One quarter of the spectrum is shown since spectrum is symmetric about $k_x = 0$ and $k_y = 0$.

waves are well resolved since the spectrum decays to zero well within the domain, even though the continuation method did not require the solution to do so. Both the wavepacket solutions and the lump solutions appear to decay algebraically to zero. We are currently exploring the possibilities of using (by continuation methods) the wavepacket solutions we have found to construct localized travelling solutions to infinite depth model equations and to model equations intermediate between those of Benney-Luke type and the full Euler.

5. Conclusion

We have shown, in a model for shallow water capillary-gravity waves, that two-

dimensional localized solitary solutions exist even in deeper water. That is, they exist for $B < 1/3$, and take the form of wavepacket solitary waves. Qualitatively, from the form of the dispersion relation, once such waves are found for $B < 1/3$, there is no reason why these waves cannot exist in infinite depth. In fact, we conjecture that two-dimensional wavepacket gravity-capillary solitary waves exist in water of infinite depth.

[The author has learned of two developments with interesting results related to this paper. Vanden-Broeck [15] has computed localized wavepacket solitary wave solutions of the full Euler equations in infinite depth, and in [6], wavepackets analogous to those described here are shown to arise from an envelope Davey-Stewartson equation. (Paragraph added after the acceptance of this manuscript for publication.)]

REFERENCES

- [1] T. R. Akylas, *Envelope solitons with stationary crests*, Phys. Fluids A, 5, 4, 789–791, 1993.
- [2] K. Berger and P. A. Milewski, *The generation and evolution of lump solitary waves in surface-tension-dominated flows*, SIAM J. Appl. Math., 61, 731–750, 2000.
- [3] W. Craig, *Nonexistence of solitary waves in three dimensions*, preprint.
- [4] F. Dias and C. Kharif, *Nonlinear Gravity and Capillary-Gravity Waves*, Ann. Rev. Fluid Mech., 31, 301–346, 1999.
- [5] M. Groves, *Fully localised solitary-wave solutions of the three-dimensional gravity-capillary water-wave problem*, preprint.
- [6] B. Kim and T. R. Akylas, *On gravity-capillary lumps*, preprint, 2004.
- [7] G. Iooss and P. Kirmann, *Capillary gravity waves on the free surface of an inviscid fluid of infinite depth - existence of solitary waves*, Arch. Rat. Mech. Anal., 136, 1–19, 1996.
- [8] M. S. Longuet-Higgins, *Capillary-gravity waves of solitary type and envelope solitons on deep water*, J. Fluid Mech. 252, 703–711, 1993.
- [9] P. A. Milewski, *Oscillating tails in the perturbed Korteweg-de Vries equation*, Studies in Appl. Math. 90, 87–90, 1993.
- [10] P. A. Milewski and J. B. Keller, *Three dimensional water waves*, Studies Appl. Math., 37, 149,66, 1996.
- [11] P. A. Milewski and J.-M. Vanden-Broeck, *Time-dependent gravity-capillary flows past an obstacle*, Wave Motion, 29, 63–79, 1999.
- [12] M. S. Longuet-Higgins and X. Zhang, *Experiments on capillary-gravity waves of solitary type on deep water*, Phys. Fluids, 31, 301–346, 1997.
- [13] R. L. Pego and J. R. Quintero, *Two-dimensional solitary waves for a Benney-Luke equation*, Phys. D, 132, 4, 476–496, 1999.
- [14] J. Satsuma and M. J. Ablowitz, *Two-dimensional Lumps in nonlinear dispersive systems*, J. Math. Physics, 20, 1496–1503, 1979.
- [15] J.-M. Vanden-Broeck, personal communication, 2004.
- [16] J.-M. Vanden-Broeck and F. Dias, *Gravity-capillary solitary waves in water of infinite depth and related free-surface flows*, J. Fluid Mech., 240, 549–557, 1992.